

# A Tunable Digitally Operated MEMS Accelerometer

Varun Kumar, Xiaobo Guo, Roozbeh Jafari, Siavash Pourkamali

Department of Electrical Engineering, University of Texas at Dallas, Richardson, Texas, USA,  
siavash.pourkamali@utdallas.edu

**Abstract**— This work presents the concept as well as fabrication and measurement results for a new MEMS accelerometer design that can be operated directly by a digital processor without the need for an analog front end. Elimination of the analog front end for such digitally operated accelerometers can significantly lower the sensor power consumption. The accelerometer consists of a proof mass and a number of parallel plate electrostatic actuators that can be turned “ON” and “OFF” in a sequential manner by a digital controller. Consequently an “ON” or “OFF” output is provided for each input condition based on an output electrode making contact with the biased proof mass. Following a simple switching algorithm, a binary search can be performed by the digital controller to find the acceleration as a binary number. This paper also demonstrates an example of such an accelerometer successfully operated in the zero to 1g range with a 2-bit resolution. The same device concept and configuration can be enhanced to higher number of bits.

**Keywords**—MEMS; digital accelerometer; low power consumption; tunable acceleration switch.

## I. INTRODUCTION

Compact, low cost, and low power accelerometers are required for numerous industrial, biomedical, geological and automotive applications that include sports watches [1], depth measurement for CPR chest compressions [2], navigation systems, vehicle crash detectors and acoustic and seismic sensors [3]. MEMS based accelerometers offering much of what is desirable for high volume applications, while providing adequate sensitivity, have become very successful commercial products and are widely used in modern integrated systems. Over the past few decades, different types of accelerometers based on various operation principles have been demonstrated. Some of the most popular detection mechanisms used in MEMS accelerometers includes piezoresistive [4], piezoelectric [5], capacitive [6], and electron tunneling readout [7]. Most commercially successful MEMS accelerometers work based on capacitive detection, which involves measuring the change in the capacitance between stationary electrodes fixed to the substrate and movable electrodes on a suspended mass. The suspended mass, also called the proof mass, has to be relatively large (typically in the millimeter range) so as to have a highly sensitive accelerometer.

In today’s modern wireless world, power consumption is one of the most essential limiting factors which directly affects the life or suitability of a sensor system. In most cases, frequent charging or replacement of the battery due to power loss is simply not feasible. With aggressive power reduction in digital electronics in recent years, MEMS sensors remain one of the most power hungry components in integrated systems. For example, Lee et al have demonstrated a wireless sensor

network (WSN) for monitoring the health and performance of motors which includes MEMS sensors, two signal processors, and the communication modules. The total nominal power consumption of the WSN is as high as 35mW, out of which close to 62% (21.6mW) is the power required for operation of the MEMS sensors, with the wireless link and signal processing unit being responsible for only close to a third of the total power consumption [8]. In most cases the large power consumption of MEMS sensors is attributed to the analog front end needed for reading, processing, and analog to digital conversion of the sensor output, which is typically responsible for most to all the power consumption of the whole sensor [9].

Therefore, significant power savings (in some cases close to zero static power consumption) can be achieved by elimination of the analog front-end. This calls for a paradigm shift in MEMS sensor design moving from analog sensors towards sensors with direct digital operation/output. In an effort to dramatically reduce the power consumption of MEMS inertial sensors, we have demonstrated a first step towards implementation of a fully digital MEMS accelerometer by digitally operating a tunable MEMS acceleration switch.

## II. OPERATING PRINCIPLE

### A. Background

Acceleration switches are simple devices with an output that can be high (ON) or low (OFF) depending on the pre-determined acceleration threshold of the device and the acceleration the device is subjected to [11]. Most acceleration switches are comprised of a suspended mass anchored to a substrate with flexible tethers. If the device is subjected to an acceleration higher than its threshold value, the suspended mass will come in contact with an electrode closing a circuit and signaling that the acceleration threshold has been reached. Hence, such devices require close to no power for operation and their output can be directly fed to a digital processor without any further processing. However, an acceleration switch can only indicate whether the applied acceleration is higher or lower than the set threshold and cannot provide quantitative information about how much acceleration is applied to the device at each moment. In other words, an acceleration switch can be referred to as a single bit digital accelerometer. The approach demonstrated in this work is to add digital control ability via electrostatic tuning to acceleration switches and turn them into multi-bit digital accelerometers. Therefore, devices shown in this work are acceleration switches that can perform quantitative acceleration measurements with the help of a digital controller.

### B. Device Structure

Figure 1 shows a simplified schematic view of a single axis

---

This work was supported by the US National Science Foundation under ECSS award #1345161 and #1314259.

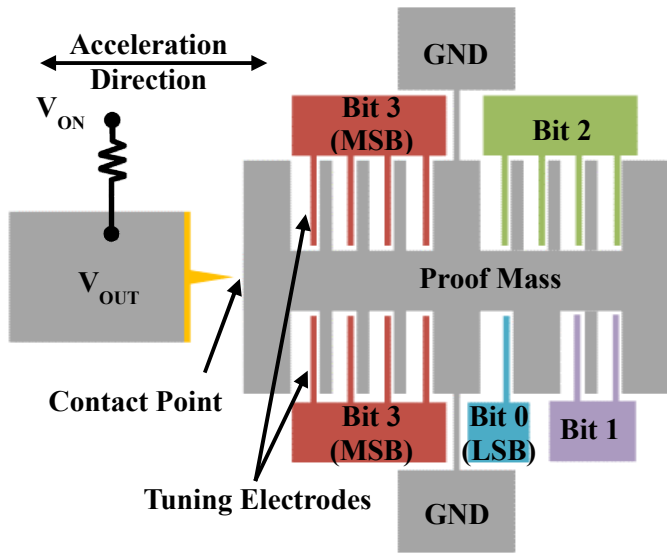


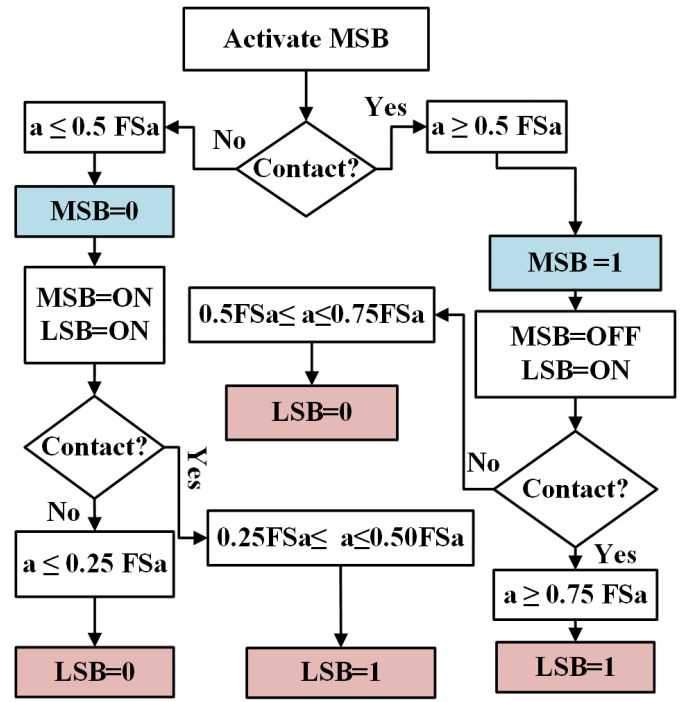
Fig. 1. Simplified schematic view of a 4-bit digitally operated accelerometer.

4-bit accelerometer operating based on the principle of an acceleration switch with digitally tunable threshold. The structure consists of a number of electrostatic tuning electrodes that can apply an assistive force to the proof-mass, thus changing its acceleration threshold over a wide range. The bulky proof mass moves back and forth in the horizontal direction as a result of the applied acceleration. The proof mass is connected to ground (GND). The stationary output electrode which is biased with a bias voltage ( $V_{ON}$ ) through a large resistor has a metallic tip that comes in contact with the proof mass once the acceleration exceeds the threshold, hence setting the output electrode voltage to zero. Application of an assistive force which pulls the proof mass towards the metallic tip will lower the acceleration threshold and vice versa. In this manner, having an arrangement of multiple electrostatic actuators with appropriate strengths (electrode finger size and number) around the proof mass and selectively turning them ON or OFF, a binary search can be performed to find the value of the applied acceleration. The mass of the proof mass and the stiffness of the tethers is to be chosen in a way that when the device is subjected to full scale acceleration and all electrode voltages are set to zero, the displacement is equal to the gap size between the metallic tip and the proof mass, i.e.:

$$K \cdot g = m \cdot a_{\max} \quad (1)$$

where  $K$  is the stiffness of the tethers,  $g$  is the gap size between the metallic tip and the proof mass,  $m$  is the mass of the proof mass and  $a_{\max}$  is the full-scale acceleration.

To perform an acceleration measurement, the tuning electrodes are to be turned ON or OFF in a sequential manner via an interfaced digital controller. Turning an electrode ON means application of a pre-determined fixed voltage to the electrode by the digital controller. The actuator associated with the most significant bit (MSB), which is Bit 3 in this case (Figure 1), has twice the number of identical parallel plate actuator fingers compared to the next most significant bit (Bit 2). In other words, Bit 3 provides an actuation force which is exactly twice that of Bit 2 when turned on. Similarly, the



a- Acceleration : FSa-Full Scale Acceleration

Fig. 2. Flowchart showing algorithm for binary search in a 2-bit digital accelerometer.

number actuator fingers goes down by a factor of two from each more significant bit to the next less significant bit and the least significant bit (Bit 0) has the minimum number of actuator fingers. The number of electrode, electrostatic actuator gap size, and electrode areas are to be chosen so that upon application of the ON voltage to the MSB actuator a force equal to 50% of the full scale acceleration force is applied to the proof mass.

### C. Binary Search for Acceleration Measurement

Figure 2 shows a sample flow-chart for performing the binary search in a 2-bit accelerometer. The binary search to find the acceleration in each measurement cycle begins by activating the MSB electrode. If the switch closes when the MSB electrode is activated, i.e. the proof mass and the metallic tip come in contact due to the activation of the MSB alone, the acceleration is larger than or equal to 50% of the full-scale acceleration. In this case, the first digit (MSB) in the digital acceleration output is "1". The MSB electrode is then turned OFF and the electrode associated with the next bit (LSB for a 2-bit accelerometer) is activated. Similarly, if this electrode alone is enough to keep the switch closed, the acceleration is above or equal to 75% of the full-scale acceleration and the second digit (LSB), will be "1" as well (2-bit binary output acceleration of 11). If there is no contact, the LSB would be "0" and the acceleration is somewhere in between 50% and 75% of full-scale (2-bit binary output acceleration of 10). In the case where the MSB doesn't initiate contact, the MSB value is "0" and it stays on while electrode associated with the next bit is actuated. In this case, if contact occurs with the LSB active, acceleration is between 25% and 50% of full-scale (2-bit binary output acceleration of 01). If with both actuators ON

contact still does not occur, then the binary output is 00 and the acceleration is below 25% of full-scale. The mapping of the binary output of such 2-bit accelerometer to the applied acceleration is as shown in Table I. The same concept and operation procedure can be enhanced to higher number of bits to realize accelerometers with higher resolutions, e.g. 4-bit, 8 bit, etc. Therefore, the acceleration amplitude with a resolution of  $1/2^n$  of full scale can be determined through  $n$  electromechanical operation steps, each of which could take hundreds of micro-seconds to a few milli-seconds depending on the design and the desired specifications.

TABLE I. MAPPING OF THE ACCELERATION BINARY OUTPUT TO THE RANGE OF THE MEASURED ACCELERATION.

MSB	LSB	Acceleration Range
0	0	$a \leq 0.25FSa^*$
0	1	$0.25FSa \leq a \leq 0.5 FSa$
1	0	$0.5FSa \leq a \leq 0.75 FSa$
1	1	$a \geq 0.75 FSa$

\*FSa-Full Scale Acceleration

### III. FABRICATION

Monocrystalline silicon with a relatively thick coating of gold was used as the structural material for the accelerometers. Figure 3 shows the fabrication process used to fabricate the devices on an SOI substrate (15  $\mu\text{m}$  thick device layer, 1 $\mu\text{m}$  thick buried oxide layer) using a two-mask micromachining process. The accelerometer silicon skeleton was first defined in the SOI device layer via deep reactive ion etching (DRIE) all the way down to the buried oxide layer (Figure 3(a)). The backside was then patterned and etched to avoid any potential stiction issues for the large proof masses. Devices were then released by removing the buried oxide layer in hydrofluoric

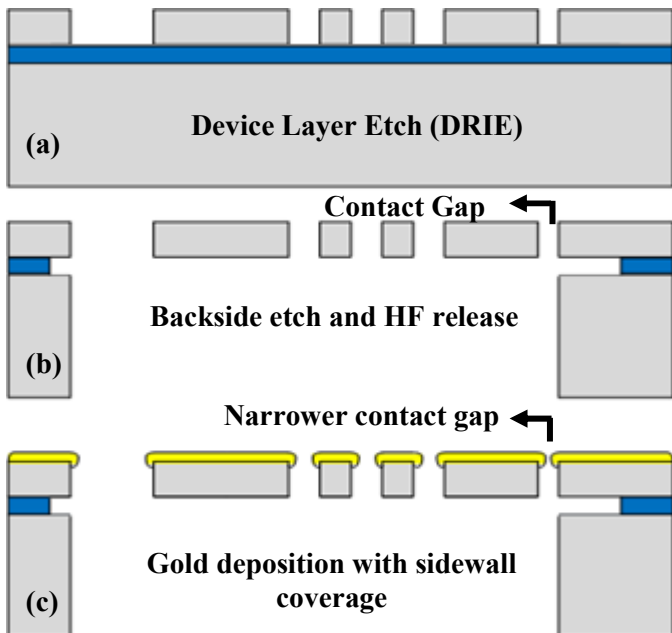


Fig. 3. Schematic cross-sectional view of the process flow.

acid (HF) (Figure 3(b)). To further narrow down the gap between the proof mass and the output electrode tip, a thick layer of gold with slight sidewall coverage was sputtered on the fabricated fully silicon devices. The sputtered gold on the sidewalls also provides a high-quality metal-metal electrical contact between the proof mass and the output electrode tip (Figure 3(c)). Thickness of the deposited gold on the sidewalls was thoroughly monitored to adjust the gap size between the contact tip and the proof mass in the deep submicron range without the need for nanolithography or any sophisticated

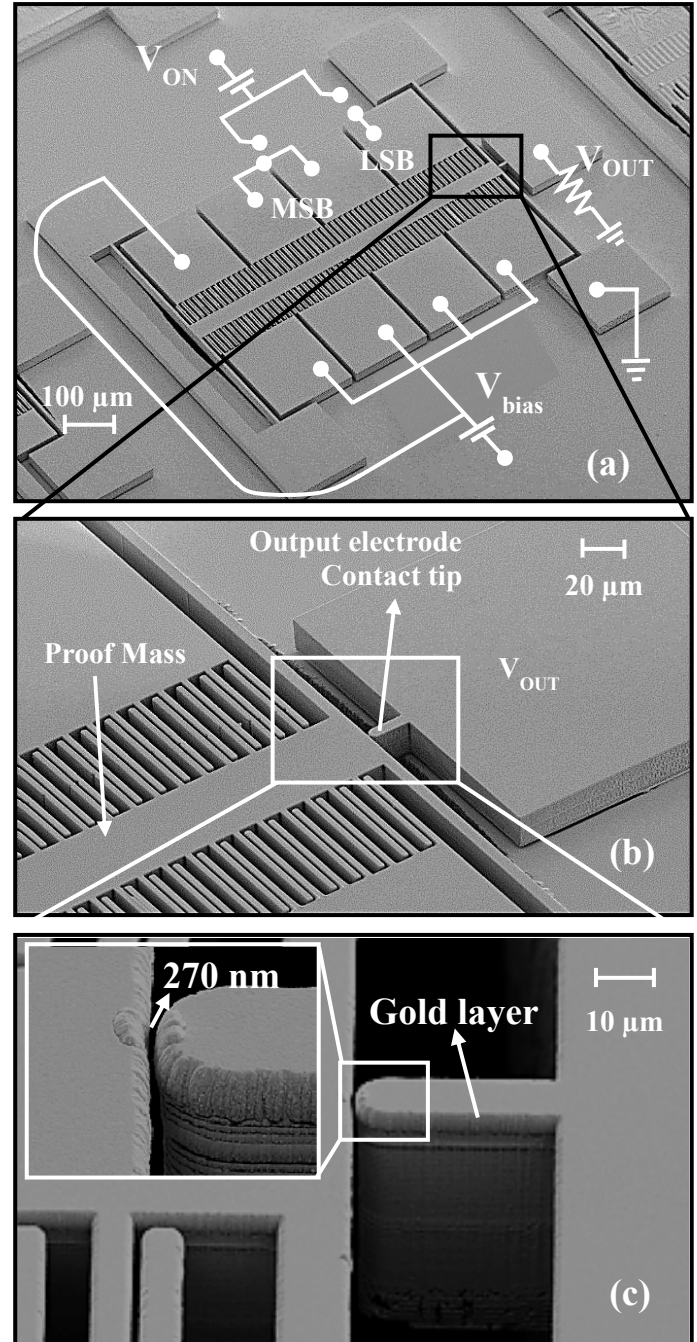


Fig. 4. (a) SEM view a fabricated digital accelerometer also showing device electrical connections for testing its performance. (b) (c) Zoomed in view of the output electrode tip area showing the narrowed down gap by gold deposition.

processing. Figure 4(a), (b) and (c) show SEM views of the digital accelerometer structure fabricated using the described fabrication sequence. Regular lithography and plasma etch constraints restrict the gap size between the proof mass and the metallic tip  $\sim 1.5\mu\text{m}$ . By depositing a thick layer of gold with side wall coverage, gap sizes as small as 270 nm were achieved (Figure 4(c)).

Eight identical electrostatic actuator finger sets are included in the device shown in Figure 4(a) allowing operation of the device as a 3-bit accelerometer with 4 of the electrodes associated with the most significant bit, 2 electrodes for the middle bit and 1 electrode for the least significant bit while the remaining electrode could be used for tuning the device operating range.

#### IV. MEASUREMENT SETUP AND RESULTS

For the specific device tested in this work, due to the relatively small proof mass and high tether stiffness, very large accelerations were required to bring the proof mass in contact with the output electrode. This would require sophisticated high-g test and characterization equipment that were not available. Therefore, to reduce the full-scale acceleration to 1g, five of the actuators were used as tuning electrodes to bring the proof mass closer to the output electrode tip. It was determined that by applying a voltage ( $V_{\text{bias}}$ ) of 47.2V to each of the five actuators (Figure 4(a)), while the other 3 actuators are OFF, an acceleration of 1g would bring the proof mass in contact with the output electrode. This sets the 11 binary output of the accelerometer to 1g, i.e. full scale acceleration of 1.33g.

The device shown in Figure 4(a) was operated in the zero to 1g range with a 2-bit resolution. The MEMS chip was placed on a printed circuit board and the acceleration was varied between zero and 1g by tilting the board with various angles with respect to the horizon. It was determined that an independent voltage ( $V_{\text{ON}}$ ) of 5.7V is to be applied to the remaining three electrodes, two of which were used as the MSB and one as the LSB.  $V_{\text{ON}}$  was applied manually to different combinations of the MSB and LSB and in each state the acceleration at which contact occurs was measured. Device performance was also validated by applying different accelerations from 0 to 1g to the device and monitoring the output while turning different bits ON or OFF. For the device tested in this work, the control signals for altering the states of the MSB and LSB were applied manually instead of using a controller for its operation.

Results of the above mentioned tests are tabulated in Table 2 showing that the device can distinguish between acceleration in the ranges of 0-0.38g, 0.38g-0.67g, 0.67g-1g, and  $\geq 1\text{g}$ , which are very close to the theoretically expected ranges. It should be noted that the full-scale acceleration in this measurement was effectively 1.33g. Although the device was never tested at accelerations higher than 1g, the transition point from output of 10 to 11, which is to occur at 1g (75% of full-scale), was successfully detected. By changing the value of  $V_{\text{bias}}$  and  $V_{\text{ON}}$ , the accelerometer full-scale value can be tuned to a wide range of accelerations. Also, it should be noted that the MSB,LSB (State) values in Table 2 indicate the required ON/OFF state for the two actuators to maintain contact over the associated acceleration range. The binary acceleration

output of the sensor that is to be provided by the digital processor is the exact opposite of the MSB,LSB actuator state.

TABLE II. MEASUREMENT RESULTS OF THE ACCELEROMETER ALONG WITH THE EXPECTED VALUES

MSB,LSB (State)	Acceleration (Theoretical) (g)	Acceleration (Measured) (g)	Binary Acceleration Output
00	$\geq 1$	$\geq 1$	11
01	$1 \geq g \geq 0.66$	$1 \geq g \geq 0.67$	10
10	$0.66 \geq g \geq 0.33$	$0.67 \geq g \geq 0.38$	01
11	$0.33 \geq g \geq 0$	$0.38 \geq g \geq 0$	00

#### V. CONCLUSION

It was demonstrated that the concept of contact-based acceleration switches can be enhanced to perform higher resolution quantitative acceleration measurements. A tunable digitally operated MEMS accelerometer with a 2-bit resolution was successfully demonstrated. A simple 2-mask fabrication process was used to fabricate the devices and the contact gap size was reduced from 1.5  $\mu\text{m}$  to 270nm by a simple maskless fabrication technique. The same device principle can be utilized to implement 6-bit, 8-bit or even higher resolution digital accelerometers. Elimination of the need for the analog front-end and analog signal conditioning can lead to significant power savings and a leap forward towards ultra-low power MEMS inertial sensors.

#### REFERENCES

- [1] Saisakul Chernbumroong, Anthony S. Atkins, and Hongnian Yu, "Activity classification using a single wrist-worn accelerometer", Proc. of the 5th International Conference on SKIMA, Benevento, pp. 1-6, 2011.
- [2] Sven O. Aase and Helge Myklebust, "Compression Depth Estimation for CPR Quality Assessment Using DSP on Accelerometer Signals", IEEE Transactions on Biomedical Engineering, Vol 49, No. 3, pp.263-268
- [3] Peter H. Veltink, Hans B. J. Bussmann, Wiebe de Vries, Wim L. J. Martens, and Rob C. Van Lummel, "Detection of Static and Dynamic Activities Using Uniaxial Accelerometers", IEEE Transactions on Rehabilitation Engineering, Vol 4, No. 4, pp.375-385, Dec 1996
- [4] Anindya Lal Roy, Tarun Kanti Bhattacharyya, "Design, Fabrication and characterization of high performance SOI MEMS piezoresistive accelerometers", Microsystem Technology, pp 55-63, 2015.
- [5] T Kobayashi, H Okada, T Masuda, R Maeda, T Itoh, "A Digital output accelerometer using MEMS-based piezoelectric accelerometers and arrayed CMOS inverters with satellite capacitors", Smart Materials and Structures, 065017, 7pp, 2011.
- [6] Xiaofeng Zhou, Lufeng Che, Shenglin Liang, Youling Lin, Xiaolin Li, Yuelin Wang, "Design and fabrication of a MEMS capacitive accelerometer with fully symmetrical double-sided H-shaped beam structure", Microelectronic Engineering, pp51-57, 2015.
- [7] V. Kumar, X. Guo, S. Pourkamali, "Single-Mask Field Emission based tunable MEMS Tunneling Accelerometer", in Press, IEEE Nano, 2015.
- [8] Lee D, "Wireless and powerless sensing node system developed for monitoring motors" Sensors pp5005-5022, 2008.
- [9] B.V. Amini and F. Ayazi, "A 2.5V 14-bit Sigma-Delta CMOS-SOI Capacitive Accelerometer," J. SSC, Dec. 2004, pp. 2467-2476.
- [10] R. Abdolvand, B.V. Amini, and F. Ayazi, "Sub-micro-gravity in-plane accelerometers with reduced capacitive gaps and extra seismic mass," IEEE Journal of Microelectromechanical Systems, Vol. 16, pp. 1036-1043, Oct. 2007.